

Altered *Hox* expression and increased cell death distinguish *Hypodactyly* from *Hoxa13* null mice

LAURA C. POST¹ and JEFFREY W. INNIS^{1, 2*}

¹Department of Human Genetics and ²Department of Pediatrics, University of Michigan, Ann Arbor, Michigan, USA

ABSTRACT *Hypodactyly* (*Hoxa13^{Hd}*) mice have a small deletion within the coding sequence of *Hoxa13* and a limb phenotype that is more severe than that of mice with an engineered null allele of *Hoxa13*. We used whole-mount *in situ* hybridization, Nile blue sulfate staining and genetic crosses to determine the basis for the phenotypic differences between these two mutants. Expression of *Hoxd13* was unaffected in *Hoxa13^{-/-}* mice, but its domain was reduced at the anterior and posterior margins of the autopod in *Hoxa13^{Hd/Hd}* limb buds. The maturation of *Hoxd11* expression was delayed and expression of *Hoxa11* failed to become restricted to the autopod/zeugopod junction in both *Hoxa13^{Hd/Hd}* and *Hoxa13^{-/-}* limb buds compared to wild-type mice. *Fgf8* expression was normal in both *Hoxa13^{Hd/Hd}* and *Hoxa13^{-/-}* mice throughout limb development. A dramatic increase in cell death was observed in limb bud mesenchyme of *Hoxa13^{Hd/Hd}* mice as early as E11.5 but not in mice homozygous for the null allele. Genetic background was excluded as the basis for the phenotypic differences. Compound heterozygotes (*Hoxa13^{-/Hd}*) displayed an intermediate phenotype relative to both homozygotes suggesting that *Hoxa13^{Hd}* has an effect on the development of the autopod beyond that which may result from a loss of HOXA13 protein. These results show that *Hoxa13^{Hd}* has a negative effect on the survival of the mesenchyme in the autopod, unlike the *Hoxa13* null mutation, that cannot be explained by a failure of the AER to express Fgfs. In addition, at least one target of HOXA13 may be *Hoxa11*.

KEY WORDS: *Hypodactyly*, *Hoxa13*, cell death, limb development

Introduction

Numerous putatively null *Hox* gene mutations have been constructed using homologous recombination (e.g. Dolle *et al.*, 1993; Small and Potter, 1993; Davis and Capecchi, 1994). Results from these studies and gain-of-function experiments indicate that *Hox* genes cooperate in regulating the growth and differentiation of specific mesenchymal condensations within their area of expression (Morgan and Tabin, 1994; Davis *et al.*, 1995; Davis and Capecchi, 1996; Goff and Tabin, 1997).

Hoxa13 is one of two vertebrate *Hox* genes in which both induced and spontaneous mutations have been studied. *Hypodactyly* (*Hoxa13^{Hd}*) is a spontaneous mouse mutation that was found to be a 50 base pair deletion within the coding sequence of exon 1 of the *Hoxa13* gene (Mortlock *et al.*, 1996). In this mutant, a stable mRNA is synthesized from the *Hoxa13^{Hd}* allele; however, the 50-nucleotide deletion introduces a translational frameshift 25 amino acids after the putative initiator methionine that would likely preclude the synthesis of a protein containing the homeodomain. Mice homozygous for this mutation have a single digit on each paw;

heterozygotes have absent or shortened first digits and other minor autopodal defects. Mice with an engineered deletion of *Hoxa13* have a different, less severe limb phenotype (Fromental-Ramain *et al.*, 1996). Homozygous null mutants have 4 digits on each paw and heterozygotes exhibit a mild alteration of the claw on the first digit.

Comparative phenotypic and molecular analyses were performed to understand the basis for the pronounced differences in the limb phenotype between mice with *Hypodactyly* or with the *Hoxa13* engineered null mutation. We examined the effects of genetic background on the limb phenotype, examined skeletons of compound heterozygotes, explored the expression of *Fgf8* and 5' *Hoxa* and *Hoxd* genes in mutant limbs, and compared the amount of cell death in developing *Hoxa13^{Hd/Hd}* and *Hoxa13^{-/-}* limb buds. Results from these experiments demonstrate that the *Hoxa13^{Hd}* allele has a negative effect on survival of the limb mesenchyme and

Abbreviations used in this paper: Hd, *Hypodactyly*; AER, Apical ectodermal ridge; FGFs, Fibroblast growth factors; BMPs, Bone morphogenetic proteins; AP, anteroposterior; PCD, programmed cell death; NBS, Nile blue sulphate.

*Address for reprints: Department of Human Genetics, University of Michigan, Ann Arbor, Michigan, 48109-0618, USA. FAX: (734) 763-3784. e-mail: innis@umich.edu

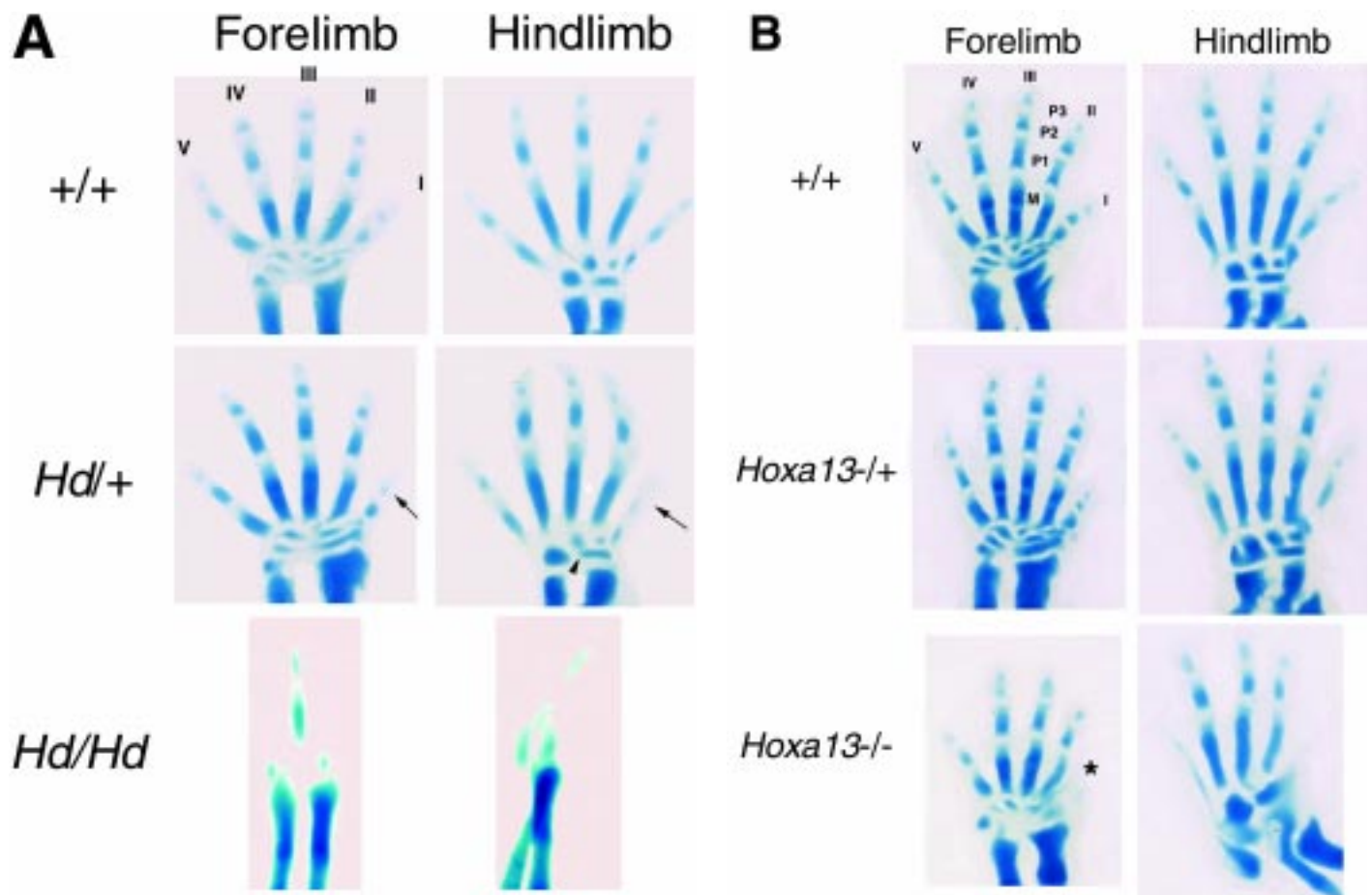


Fig. 1. Analysis of effect of genetic background on *Hoxa13^{Hd}* and the *Hoxa13* null allele. Skeletons were stained with Alizarin red and alcian blue. **(A)** E14.5 skeletons of *+/+*, *Hoxa13^{Hd/+}*, and *Hoxa13^{Hd/Hd}* mice on the alternate, 129/Sv, background. Heterozygotes have a shortened digit I (arrow) and homozygotes have only a single central digit. Cuneiform 3 and navicular lunata tarsals are incompletely segmented (arrowhead), suggesting that fusion of these elements could occur at later stages. **(B)** E15.5 skeletons of *+/+*, *Hoxa13^{+/-}*, and *Hoxa13^{-/-}* mice on the alternate BL6/C3HFe background. Heterozygotes are missing digit I except for a rudimentary condensation in the forelimb (asterisk). No differences were observed in the skeletal phenotype of either mutation on the alternate genetic background compared with the reported defects on the parental backgrounds. Digits are labeled with roman numerals. Metacarpal (M) and phalanges (P1-P3) are labeled.

on *Hoxd13* expression that cannot be explained solely by loss of *HOXA13* protein.

Results

Genetic background does not account for phenotypic differences

One hypothesis for the differences observed between *Hoxa13^{Hd}* mice and mice carrying the null allele is that genetic background (BL6/C3HFe for *Hoxa13^{Hd}* and 129/Sv for *Hoxa13^{-/-}*) modifies the morphogenetic consequences of each mutation. To test for effects due to strain differences, each mutation was crossed onto the alternate background and the skeletons of offspring from heterozygous F_1 intercross matings were analyzed.

The *Hoxa13^{Hd}* phenotype has been reported previously (Hummel, 1970; Innis *et al.*, 1996; Mortlock *et al.*, 1996). *Hoxa13^{Hd/+}* mice have a variable shortening of the first digit (ranging from missing nail to loss of both phalanges), alterations in the timing of maturation of specific bones within the autopod, and fusions of the d1-d2/c carpals and cuneiform 3-navicular tarsals. *Hoxa13^{Hd/Hd}* mice have a single digit (corresponding to digit IV) and loss or hypoplasia

of most carpals and tarsals at every stage examined. Skeletal stains of E14.5 heterozygous and homozygous *Hoxa13^{Hd}* embryos on the alternate 129/Sv^J background are shown in Figure 1A. On this alternate background, the *Hoxa13^{Hd/+}* mice exhibit shortening of the first digit compared with wild-type skeletons (arrows, $n=6$). In addition, the condensations corresponding to cuneiform 3 and navicular tarsals are not clearly separated (arrowhead; 10 of 12 hindlimbs), in contrast to *+/+* limbs at this stage, consistent with the potential for fusion between these two elements in *Hoxa13^{Hd}* mice at a later stage of development. *Hoxa13^{Hd/Hd}* skeletons have only one visible digital condensation and a reduced number of carpals and tarsals ($n=8$). These abnormalities are consistent with the previously reported phenotype of *Hoxa13^{Hd}* mutant embryos on the BL6/C3HFe background (Hummel, 1970; Mock *et al.*, 1987; Mortlock *et al.*, 1996; Robertson *et al.*, 1996), indicating little, if any, phenotypic modification by the 129/Sv^J background.

The effect of the BL6/C3HFe alternate genetic background on the *Hoxa13* null mutation was explored first by gross examination. On the parental background (129/Sv), the *Hoxa13^{-/+}* adult mice exhibit shortening and abnormal ventral bending of the nail of digit I,

sympalangism (fusion of the phalanges) of digit I, and fusion of the soft tissue of digits II and III (Fromental-Ramain *et al.*, 1996). *Hoxa13*^{-/-} embryos form only a rudimentary condensation in the forelimb corresponding to digit I, no digit I condensation in the hindlimb, and the formation of condensations of the other digital anlagen is delayed. In addition, forelimb digits II and V and all hindlimb digits lack the second phalanx, and carpal and tarsal elements are poorly defined. The soft tissue defects between *Hoxa13*^{-/-} adults on the parental (129/Sv) or mixed BL6/C3HFe backgrounds were compared (Table 1). Soft tissue fusions were observed in 9/11 mice (82%) generated by intercrossing *Hoxa13*^{+/-} animals (parental background); the other 2 animals had a malformed claw of digit I only. Of the 9 animals with fusions, 7 were bilateral, 2 affected the left hindlimb only, though one of these unilateral cases included digit IV as well as II and III. When the *Hoxa13* null mutation was crossed onto the alternate BL6/C3HFe mixed background, only 21/39 mice exhibited soft tissue fusions (54%). Of these, 13 were unilateral with a preference for involvement of the left limb (9/13). The limb phenotype in the remaining mice (18/39) was limited to a malformed claw of digit I. In all cases, the extent of fusion was variable and differences in the extent of left versus right side involvement were observed.

The skeletal phenotype of the *Hoxa13* null mutation on the alternate BL6/C3HFe background was analyzed in embryos (Fig. 1B). Homozygous mutant embryos on the alternate background (n=2) lack digit I except for a small rudiment in the forelimb (asterisk, Fig. 1B), lack the second phalanx of digits II and V in the forelimb, and lack the second phalanx in all digits in the hindlimb. In addition, the carpals and tarsals were poorly defined. Finally, digit V in the hindlimb is thin and not clearly separated from the tarsals. This phenotype was similar to what was observed on the parental, 129/Sv, genetic background (L. Post, data not shown; Fromental-Ramain *et al.*, 1996).

There was no significant difference in the phenotype of *Hoxa13*^{Hd/+} or *Hoxa13*^{Hd/Hd} mouse limbs when crossed to the 129/

TABLE 1

COMPARISON OF HOXA13^{+/-} ADULT LIMB PHENOTYPE ON THE PARENTAL (129/SV) OR ALTERNATE (BL6C3HFE) GENETIC BACKGROUND

	Parental background	BL6/C3HFe background
Soft Tissue Fusions, Digits II-III:	9	21
Bilateral	7	8 (1)
Unilateral	2 (1)	13
Left	2	9 (5)
Right	0	4 (1)
Malformed Claw Only, Digit I:	2	18
Total:	11	39

The number of animals with each defect is listed. All animals with soft tissue fusions also exhibited malformation of the claw of digit I. Numbers in parentheses indicate the number of animals who also had involvement of digit IV in the fusions.

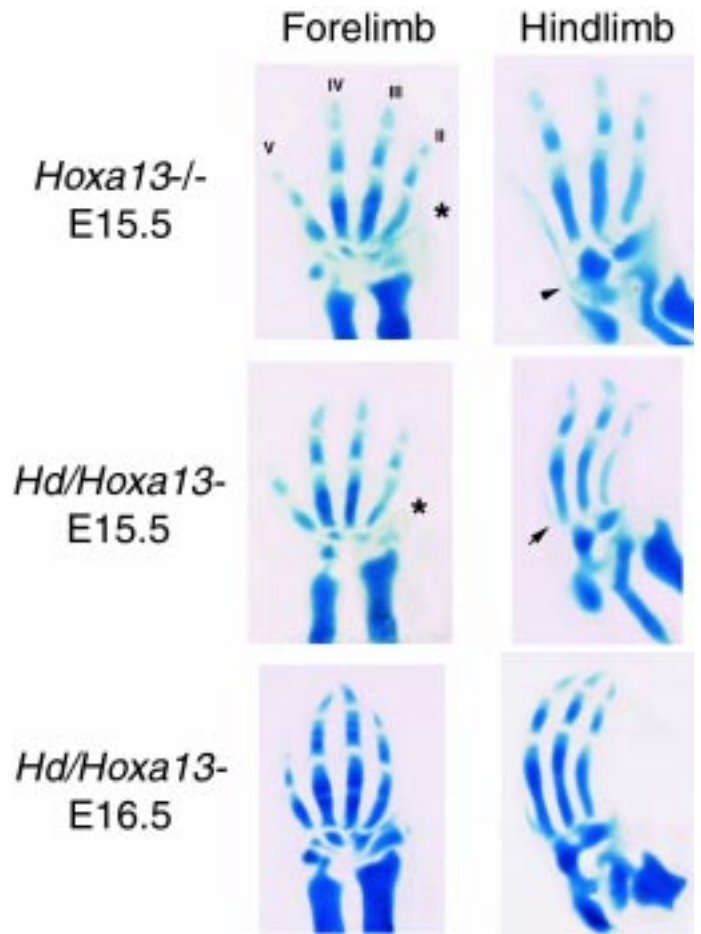


Fig. 2. Comparison of skeletal phenotype between *Hoxa13*^{-/-Hd} compound heterozygotes and *Hoxa13*^{-/-} mice. The rudimentary condensation of digit I in the forelimb is missing in the compound heterozygotes (asterisk). In the hindlimb, digit V is reduced in size and articulates with metatarsal IV (arrow) rather than with the processus trochlearis (arrow-head). In addition, all hindlimb digits exhibit an anterior bending.

Sv^J genetic background. *Hoxa13*^{+/-} adults exhibited less severe soft tissue fusions when placed on a mixed BL6/C3HFe background. This alteration was limited to heterozygotes, as the limb phenotype of *Hoxa13*^{-/-} mice on the BL6/C3HFe background was the same as that reported for the parental strain.

Embryonic limb phenotype of compound heterozygotes

Given that steady-state *Hoxa13*^{Hd} mRNA levels are normal in abundance (Mortlock *et al.*, 1996), its translation would be predicted to lead to a frameshift resulting potentially in the production of a protein without a homeodomain. Therefore, *Hoxa13*^{Hd} would likely act as a functionally null allele of *Hoxa13* and compound heterozygotes (*Hoxa13*^{-/Hd}) should have a phenotype similar to *Hoxa13*^{-/-} mice.

As a test of allelism and to explore the phenotype of compound heterozygotes, *Hoxa13*^{+/-} males were bred with *Hoxa13*^{Hd/+} females and embryos were examined for skeletal defects. From these matings, approximately 15% (8/55) of the embryos generated were compound heterozygotes as determined by genotype analysis. This is lower than the predicted 25%, but not unexpected given the fetal lethality associated with both *Hoxa13*^{Hd} and the *Hoxa13* null

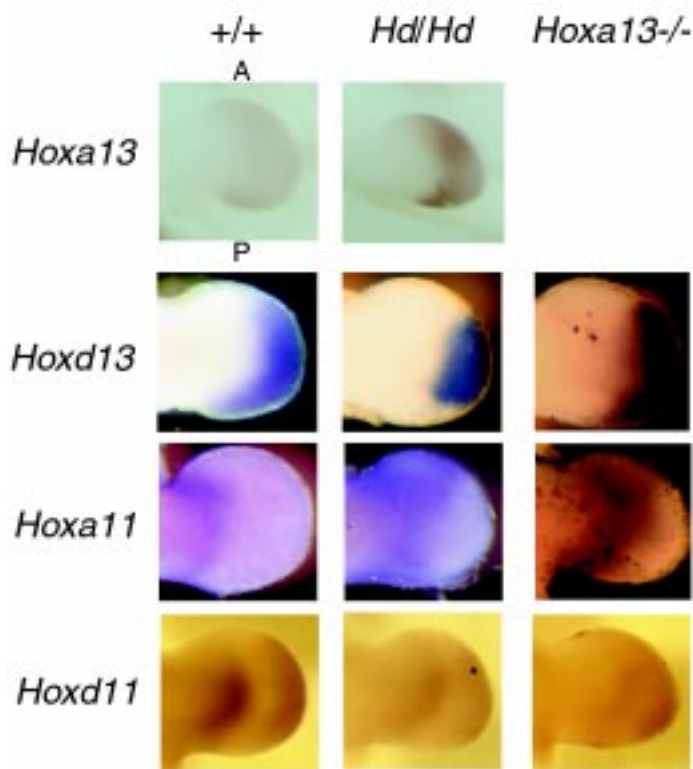


Fig. 3. Whole-mount *in situ* hybridizations of E11.5 embryos with 5' *Hox* genes. Right forelimbs hybridized with probes specific for *Hoxa13*, *Hoxd13*, *Hoxa11* or *Hoxd11*. *Hoxa13* transcripts are detected in *Hoxa13^{Hd/Hd}* embryos, possibly at higher levels. *Hoxd13* expression is reduced at both the anterior and posterior margins in *Hoxa13^{Hd/Hd}* embryos, but is not altered in *Hoxa13^{-/-}* embryos. *Hoxa11* expression fails to become restricted to the autopod/zeugopod junction in both mutants resulting in increased expression in the anterior and distal autopod. There is a slight delay in the alteration of *Hoxd11* expression from a single, broad domain to two stripes in both mutants. All images are dorsal views of right forelimbs. A, anterior; P, posterior.

allele at the late gestational ages we examined (E15.5 and E16.5; Post and Innis, unpublished observations; Fromental-Ramain *et al.*, 1996). Furthermore, there was a direct correlation between defects and genotype for both homozygous mutants and for compound heterozygotes. Representative skeletons of two *Hoxa13^{-/-}* embryos (E15.5) and several *Hoxa13^{-Hd}* compound heterozygotes (1 embryo at E15.5, 3 embryos at E16.5) are shown in Figure 2. Skeletons of *Hoxa13^{-/-}* and *Hoxa13^{-Hd}* both fail to develop digit I, the second phalanx of digits II and V of the forelimb, and the second phalanx of all of the remaining four digits in the hindlimb. However, several morphological differences were observed in *Hoxa13^{-Hd}* skeletons that were not observed in any *Hoxa13^{-/-}* animals in our study. In the forelimb, the rudimentary condensation in *Hoxa13^{-/-}* mice corresponding to digit I never formed in the compound heterozygote (asterisk, Fig. 2). *Hoxa13^{-/-}* mice have a second phalanx in forelimb digits II and III; however, in *Hoxa13^{-Hd}* mice, these condensations were not observed at both E15.5 and E16.5. Digit V is dramatically shorter in the hindlimbs of *Hoxa13^{-Hd}* mice than in *Hoxa13^{-/-}* (arrow, Fig. 2) and it articulates with the metacarpal of digit IV rather than the processus trochlearis (arrowhead, Fig. 2). At E15.5, hindlimb digit II is thinner and the tarsals are

smaller in *Hoxa13^{-Hd}* mice. By E16.5 these bones in *Hoxa13^{-Hd}* mice more closely resemble the E15.5 *Hoxa13^{-/-}* limb, suggesting a further delay in growth in the compound heterozygote. Finally, hindlimb digits II and III in *Hoxa13^{-/-}* mice exhibit a mild abnormal bending toward the anterior side at E14.5 and E15.5. In every compound heterozygote examined, all hindlimb digits exhibited this unusual anterior bending (n=4 mice). The similarities between *Hoxa13^{-/-}* mice and the compound heterozygotes support our previous conclusion that *Hoxa13^{Hd}* is an allele of *Hoxa13* (Mortlock *et al.*, 1996). The differences observed between *Hoxa13^{-Hd}* and *Hoxa13^{-/-}* are minor, yet are similar in degree to those seen between the individual heterozygous mutants (see Fig. 1).

***Hox* gene expression in mutants**

Most single *Hox* gene null mutations result in alteration in patterning (e.g. Morgan *et al.*, 1992; Condie and Capecchi, 1993); loss of structure is often observed when two or more null alleles are combined (Condie and Capecchi, 1994; Davis *et al.*, 1995; Rijli *et al.*, 1995). One explanation for the more severe *Hoxa13^{Hd}* phenotype is that *Hoxa13^{Hd}* causes functional loss or misexpression of other *Hox* genes necessary for proper formation of the autopod. To test this hypothesis, whole-mount *in situ* hybridization was performed to examine *Hox* gene expression in *Hoxa13^{Hd/Hd}* and *Hoxa13^{-/-}* E11.5 limb buds (Fig. 3). Sense controls for all probes were negative (data not shown). *Hoxa13* expression was maintained in a normal distribution in *Hoxa13^{Hd/Hd}* embryos at E11.5 (n=3).

The normal expression domain of *Hoxd13* extends across the entire anteroposterior (AP) axis of the distal autopod at E11.5 (Dolle *et al.*, 1991; Fig. 3). This domain was reduced at the anterior and posterior margins in *Hoxa13^{Hd/Hd}* limbs at (n=4) and remained smaller at E12.5 (n=4, data not shown) indicating that this reduction was not simply the result of a developmental delay in the establishment of the expression domain. Expression of *Hoxd13* in *Hoxa13^{-/-}* limbs is not significantly altered compared to wild-type embryos (n=3).

Hoxa11 expression in wild-type mice is first detected across most of the autopod except for a small area at the posterior distal tip and by E11.5 has become restricted to a narrow stripe corresponding to the autopod/zeugopod junction (Haack and Gruss, 1993; Small and Potter, 1993; Fig. 3). In both *Hoxa13^{Hd/Hd}* and *Hoxa13^{-/-}* E11.5 embryos (n=4 for each mutation), the expression domain is abnormally maintained throughout much of the developing autopod. These data suggest that one function of *Hoxa13* may be to repress *Hoxa11* expression in the distal autopod.

Hoxd11 expression begins as a broad domain encompassing most of the autopod and by E11.5 becomes restricted to two stripes along the AP axis in normal mice (Davis and Capecchi, 1994; Fig. 3). In E11.5 *Hoxa13^{Hd/Hd}* (n=4) and *Hoxa13^{-/-}* (n=3) embryos, this restriction is delayed, suggesting that the proper timing of the establishment of *Hoxd11* expression is dependent upon *Hoxa13*.

***AER* function is unaffected in both mutants**

Fibroblast growth factors from the apical ectodermal ridge (AER) are important for outgrowth of the limb bud along the proximal-distal axis (Summerbell *et al.*, 1973; Niswander *et al.*, 1993; Fallon *et al.*, 1994). Another potential explanation for the loss of structure in *Hoxa13^{Hd}* mice could be that the AER is not maintained during development leading to loss of expression of Fgfs. This hypothesis was tested by examining the expression of

Fgf8 in both *Hoxa13^{Hd/Hd}* and *Hoxa13^{-/-}* limb buds by whole-mount *in situ* hybridization (Fig. 4). *Fgf8* is expressed in the AER along the entire AP axis for the entire time in which the ridge is an identifiable structure (Crossley and Martin, 1995). At E11.5 in limbs of both *Hoxa13^{Hd/Hd}* (n=1) and *Hoxa13^{-/-}* (n=3) mutants, *Fgf8* expression is indistinguishable from wild-type embryos (Fig. 4A). At E14.5, low levels of *Fgf8* expression are detected at the distal tips of the developing digits in the hindlimbs of wild-type mice (n=2). This expression pattern is maintained in the single digit of *Hoxa13^{Hd/Hd}* hindlimbs (n=2, arrowheads, Fig. 4B). Therefore, AER function as determined by *Fgf8* expression is apparently unaffected in *Hoxa13^{Hd}* mice, suggesting that the digital loss cannot be attributed to a primary failure of the AER.

Nile blue sulphate staining reveals an increase in cell death in *Hoxa13^{Hd/Hd}* limb buds

Limb patterning is the result of growth coupled with selected programmed cell death (PCD). Several areas of the developing limb (anterior and posterior necrotic zones and the interdigital areas) are known to undergo PCD (Milaire, 1992, and references therein). Reduction in the amount of PCD may result in polydactyly; increased cell death may lead to loss of structures. To determine whether digital loss was secondary to increased cell death, Nile blue sulphate (NBS) staining of *Hoxa13^{Hd/Hd}* and *Hoxa13^{-/-}* embryos was performed. At E11.5, no observable staining is apparent in *+/+* limb buds (n=3), but a narrow domain of stained cells is observed in *Hoxa13^{Hd/Hd}* limb buds in the mesenchyme under the AER (n=2, arrowheads, Fig. 5A). At E12.5, the anterior and posterior necrotic zones are visible in *+/+* limb buds (n=5, Fig. 5B). However, the amount of cell staining in *Hoxa13^{Hd/Hd}* embryos has increased and extends to mesenchyme more proximal to the progress zone (n=1, Fig. 5B). Increased cell death was never observed in the AER. One area in the central portion of the autopod has fewer NBS-stained cells and may correspond to the tissue that will give rise to the single digit in these animals. Limb buds of *Hoxa13^{-/-}* mice at E12.5 (n=3) are indistinguishable from wild-type mice (Fig. 5B). Therefore, increased cell death in the autopod is responsible for the severe loss of tissue associated with the *Hoxa13^{Hd}* mutation.

Discussion

Analysis and comparison of the effects of multiple alleles are useful to obtain a better understanding of gene function. In this paper, we have explored the basis for the dramatic phenotypic differences that result from two different mutations in the *Hoxa13* gene, *Hoxa13^{Hd}* and *Hoxa13* null mice constructed by homologous recombination. The effect of genetic background on the phenotype was tested by crossing *Hoxa13^{Hd}* and the *Hoxa13* null mutation onto the alternate backgrounds. Analysis of skeletons from these matings revealed no significant differences between the observed defects and those reported for each mutation (Fig. 1A and B). However, the soft tissue defects observed in *Hoxa13^{-/+}* animals appeared to be less severe on a mixed, 129/B6C3Fe background than on the original 129/Sv strain (Table 1). These data suggest that a reduced amount of HOXA13 protein can affect the final morphology of the digits, but that this activity can be influenced to a degree by other factors within the genetic background. However, in the complete absence of normal protein, the dramatic phenotypic differences observed between

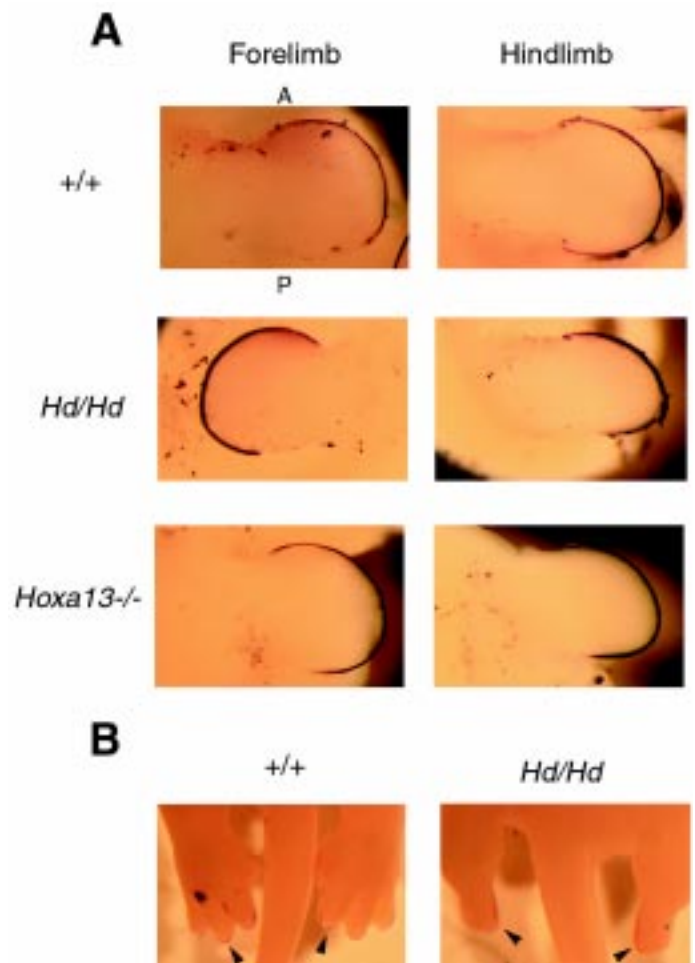


Fig. 4. Whole-mount *in situ* hybridization of *Fgf8* in *Hoxa13^{Hd/Hd}* and *Hoxa13^{-/-}* embryos. All images are dorsal views of right limbs except *Hoxa13^{Hd/Hd}* forelimb (left limb). (A) *Fgf8* expression is not altered in either mutation at E11.5. (B) Expression is maintained at the distal ends of the digits in *+/+* embryos at E14.5 and at the end of the single digit in *Hoxa13^{Hd/Hd}* embryos (arrowheads). Images are dorsal views of the hindlimbs. A, anterior; P, posterior.

Hoxa13^{Hd} mice and *Hoxa13^{-/-}* mice cannot be explained by genetic background alone.

To test whether the *Hoxa13^{Hd}* mutation results in a null allele of *Hoxa13*, compound heterozygotes (*Hoxa13^{-/Hd}*) were generated (Fig. 2). The similarities observed between *Hoxa13^{-/Hd}* and *Hoxa13^{-/-}* skeletons confirmed that *Hoxa13^{Hd}* is clearly an allele of *Hoxa13*; however, the intermediate phenotype observed in the compound heterozygotes indicates that the *Hoxa13^{Hd}* mutation has an additional effect on limb development besides the loss of HOXA13 function.

Robertson *et al.* (1996) reported an increase in cell death of limb mesenchyme in *Hoxa13^{Hd/Hd}* embryos. In our studies, increased cell death was observed in limbs of *Hoxa13^{Hd/Hd}* embryos, but not *Hoxa13^{-/-}* embryos, at both E11.5 and E12.5 (Fig. 5) and encompasses most of the autopod except for a small area within the central core of the bud. This area of surviving tissue presumably gives rise to the single digit that later forms in *Hoxa13^{Hd/Hd}* mice. These results suggest that different mechanisms are responsible for the limb defects associated with each mutation. In *Hoxa13^{Hd/Hd}*

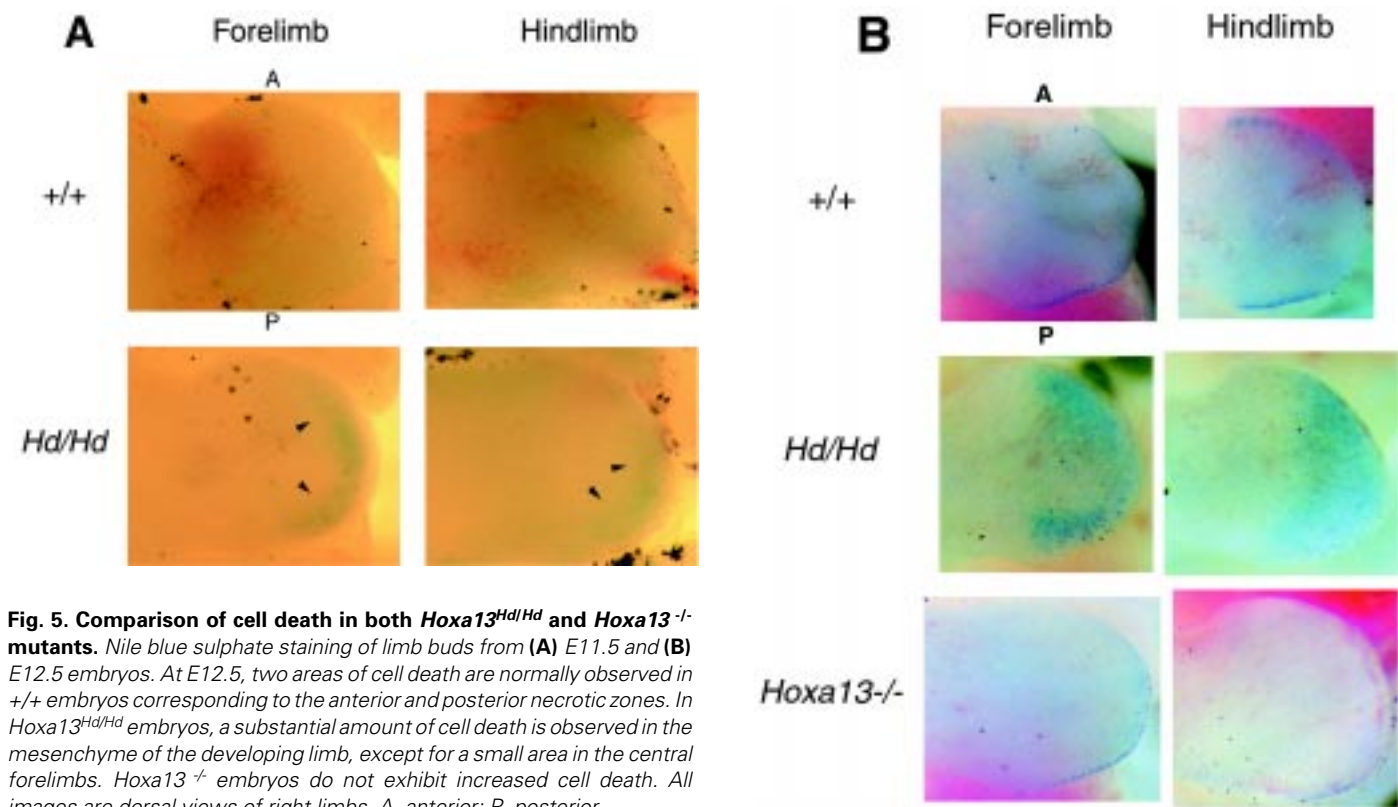


Fig. 5. Comparison of cell death in both *Hoxa13^{Hd/Hd}* and *Hoxa13^{-/-}* mutants. Nile blue sulphate staining of limb buds from (A) E11.5 and (B) E12.5 embryos. At E12.5, two areas of cell death are normally observed in *+/+* embryos corresponding to the anterior and posterior necrotic zones. In *Hoxa13^{Hd/Hd}* embryos, a substantial amount of cell death is observed in the mesenchyme of the developing limb, except for a small area in the central forelimbs. *Hoxa13^{-/-}* embryos do not exhibit increased cell death. All images are dorsal views of right limbs. A, anterior; P, posterior.

embryos, tissue is formed early but undergoes cell death. In *Hoxa13^{-/-}* embryos, loss of digit I and phalangeal elements are not caused by excessive cell death, but rather by a reduction in the proliferation of distal mesenchyme, leaving fewer cells available to undergo condensation and differentiation (Fromental-Ramain *et al.*, 1996). The presumed loss of normal HOXA13 protein in *Hoxa13^{Hd/Hd}* limbs may also contribute to poor digital development. The differential increase in cell death provides further molecular evidence that the *Hoxa13^{Hd}* mutation has a deleterious effect on limb formation beyond a simple loss of function of HOXA13 protein.

Limb truncation can also occur when AER function is disrupted (Saunders, 1948; Summerbell, 1974). *Fgf8* expression was examined as a marker for the AER and no significant alterations were observed between wild-type limb buds and those of *Hoxa13^{Hd/Hd}* or *Hoxa13^{-/-}* mice at E11.5 (Fig. 4). At later stages, *Fgf8* expression, and therefore AER integrity, was unaltered in *Hoxa13^{Hd/Hd}* limb buds compared to wild-type mice. *Fgf4*, which is downregulated prior to AER regression, was shown to be expressed longer in hindlimbs of *Hoxa13^{Hd/Hd}* embryos compared with wild-type limb buds (Robertson *et al.*, 1997). Taken together, these data suggest that growth factors are generated from the AER of both *Hoxa13^{Hd}* and *Hoxa13^{-/-}* mutants and are available to stimulate the underlying mesenchyme to proliferate. However, in *Hoxa13^{Hd}* mice, there is an increase in cell death in the distal limb mesenchyme. It is possible that the growth factors are not properly received by the underlying mesenchyme, or the signal cannot be transmitted properly to the cells. Robertson *et al.* (1996) observed gaps between the AER and the underlying mesenchyme in some

Hoxa13^{Hd/Hd} limb buds, suggesting that the ectoderm and mesoderm may lose direct contact in these mutants. Alternatively, the growth factor receptors or interacting extracellular matrix molecules needed for growth factors to bind their receptors are not expressed properly in the mesenchyme of *Hoxa13^{Hd/Hd}* limbs.

BMP function is directly involved in cell death in the limb (Ganan *et al.*, 1996; Yokouchi *et al.*, 1996; Macias *et al.*, 1997). In addition, BMPs have recently been demonstrated to promote AER regression (Pizette and Niswander, 1999). The prolonged maintenance of the AER in *Hoxa13^{Hd}* mice found by Robertson *et al.* (1996) suggests that BMP or mesenchymal function in relation to AER regression may be impaired in these animals.

Alterations in the expression patterns of the 5' *Hox* genes described may also contribute to the severe phenotype in *Hoxa13^{Hd}* mice. The expression of *Hoxd13* was differentially altered between the two mutations at E11.5. In *Hoxa13^{-/-}* embryos, the pattern of *Hoxd13* expression is largely normal and spans the entire AP axis of the distal autopod. However, in *Hd/Hd* embryos, expression of *Hoxd13* is reduced at both the anterior and posterior boundaries (Fig. 3, this paper; Robertson *et al.*, 1997). This restriction is maintained at E12.5 indicating that it is not just the result of a developmental delay. This central expression domain roughly corresponds to the small area of surviving cells in these limbs. However, it is not clear whether the survival of this tissue allows the expression of *Hoxd13* or the expression of *Hoxd13* in this area inhibits cell death. *Hoxa13* expression is normal in *Hoxa13^{Hd/Hd}* mutant limb buds even in areas undergoing cell death, so the mere presence of increased cell death is not necessarily sufficient to explain the

narrower *Hoxd13* domain. *Hoxa11* expression fails to become restricted in both *Hoxa13^{Hd/Hd}* and *Hoxa13^{-/-}* mutants to a similar degree (Fig. 3). The effect of prolonged *Hoxa11* expression in the autopod is unknown. These results suggest that HOXA13 is necessary for the exclusion of *Hoxa11* from the distal autopod and provides evidence in support of *Hoxa11* as a potential transcriptional target of *Hoxa13*. *Hoxa13* RNA (mutant form) is expressed in *Hoxa13^{Hd/Hd}* limb buds in a normal domain, but at higher levels compared with wild-type mice. The increase in expression, albeit minor, was confirmed by Northern analysis (data not shown). Therefore, HOXA13 may negatively regulate its own steady-state expression levels.

In the complete absence of the limb-specific group 13 *Hox* genes (*Hoxa13^{-/-}/Hoxd13^{-/-}*), embryos have a single, long condensation extending from the ulna but nothing resembling additional carpals (Fromental-Ramain *et al.*, 1996). *Hoxa13^{-/-}* mice have four digits (Fromental-Ramain *et al.*, 1996) and even mice heterozygous for *Hoxa13*, but lacking *Hoxd11*, *Hoxd12*, and *Hoxd13* (*Hoxd^{del/del}/Hoxa13^{-/+}*, Zakany *et al.*, 1997) have four digits, although they are short and poorly defined. Therefore, one copy of *Hoxa13*, even in the complete absence of 5' *Hoxd* genes, is sufficient to form carpals, tarsals, and digital elements. How, then, does *Hoxa13^{Hd}* lead to such a severe reduction in the formation of these same elements? Given that RNA is produced from the *Hoxa13^{Hd}* allele, a mutant protein could be generated that may contribute to the deleterious effects of this mutation on limb patterning. Work is in progress to explore this hypothesis.

Materials and Methods

Breeding and skeletal staining

Hypodactyly mice were obtained from The Jackson Laboratory where the mutation is carried on a BL6/C3HFe F₁ hybrid. It has been carried in our laboratory by intercrossing *Hoxa13^{Hd/+}* mice; consequently, the contribution of BL/6 and C3HFe varies in each mouse. Despite this mixed background, the *Hoxa13^{Hd}* phenotype in these animals remains very similar. The engineered null mutation of *Hoxa13* (*Hoxa13^{-/-}*) was generated in 129/Sv ES cells, and heterozygous mutants were mated to C57BL/6J or 129/Sv mice as previously described (Fromental-Ramain *et al.*, 1996). The degree of BL/6J genetic contribution in these animals is not precisely known. Two null alleles were constructed, one in which the homeodomain was interrupted by insertion of a neomycin cassette and one in which the entire *Hoxa13* locus was replaced with the neomycin cassette. *Hoxa13* mutant mice missing the entire locus were used in our experiments. Control skeletons (each mutation on its parent background) were generated by timed matings of heterozygous mutants; the morning after mating was designated gestational age E0.5. To test the effect of genetic background, wild-type females from our colony (B6C3Fe) were mated with *Hoxa13^{-/+}* males and *Hoxa13^{Hd/+}* females were mated with +/+ 129/Sv^l males (kindly provided by J. Karolyi). Heterozygous mutant F1 sibling mice were intercrossed. Compound heterozygotes were generated by timed matings between *Hoxa13^{Hd/+}* females with *Hoxa13^{-/+}* males. Live embryos were isolated for each genotype at every stage examined. At the designated gestational ages, embryos were dissected in PBS and yolk sacs were removed for genotyping. The limbs from each embryo were removed and stained with Alizarin red and alcian blue as described (Kimmel and Trammel, 1981) for 4 days to 1 week. Limbs were then cleared in 2% KOH for approximately 24 h and subsequently passed through increasing concentrations of glycerol before storage in 100% glycerol. All mouse experiments were carried out under approval of the University of Michigan University Committee on Use and Care of Animals.

DNA isolation and PCR analysis

DNA isolation and genotyping for the *Hoxa13^{Hd}* allele was performed as described previously (Miller *et al.*, 1988; Mortlock *et al.*, 1996). Genotyping for the engineered *Hoxa13* null mutation required separate reactions to detect the wild-type and mutant alleles. The reaction mixture for the wild-type allele included 100 ng DNA, 50 mM KCl, 10 mM Tris (pH 8.3), 1.5 mM MgCl₂, 200 μM dNTPs, 150 ng primer #4693H (5'-TCGTGGCAAAGAGCAATCAG-3'), 150 ng primer #4695H (5'-TTGTGTGTTTTAGGGGCTGATGAGT-3'), 2.5 μg BSA, and 1.5 U Taq polymerase (Gibco-BRL). The reaction mixture for the mutant allele was identical except that primer #4694H (5'-TGCATACGCTTGATCCGGCTACCTG-3') was used in place of #4693H. Cycling conditions were 94°C, 1 min; 62°C, 1.5 min; 72°C, 2.5 min for 2 cycles, then 30 cycles as above except the denaturation temperature was reduced to 92°C. A final extension step was performed at 72°C for 8 min. Amplified products of 620 bases (wild-type allele) or 500 bases (null allele) were visualized by 2% agarose gel electrophoresis.

Whole-mount *in situ* hybridization

Embryos at designated gestational ages were fixed in 4% paraformaldehyde for 4 h at 4°C, washed 3 times in PBST (1xPBS+0.1% Tween-20), and dehydrated through increasing concentrations of methanol. Whole-mount *in situ* hybridizations with digoxigenin-labeled RNA probes were carried out as described (Conlon and Herrmann, 1993). The antisense probe specific for *Hoxa13* is 900 base pairs (Nco I-Pst I fragment) of the 3' untranslated region between the homeobox and first polyadenylation signal (Mortlock *et al.*, 1996). *Hoxd11* and *Hoxd13*, *Hoxa11*, and *Fgf8b* probes were gifts of D. Duboule, S. Potter, and G. Dressler respectively.

Analysis of cell death

Cell death was assayed by Nile blue sulphate staining. E11.5 and E12.5 embryos from *Hoxa13^{Hd/+}* or *Hoxa13^{-/+}* heterozygous matings were dissected in PBS pre-warmed to 37°C. Yolk sacs were removed for genotype analysis. Embryos were rinsed twice in pre-warmed PBS, and then incubated in 0.005% Nile blue sulfate (Sigma) in PBS at 37°C for 30 min. They were then rinsed once in pre-warmed PBS and incubated overnight at 4°C. Limbs were photographed the following day using a Leica MZ8 dissecting microscope and camera.

Acknowledgments

We wish to thank Jason Moore for extensive statistical analysis of skeletons. *Hoxa13* null mice were generously provided by Catherine Fromental-Ramain and Xavier Warot. We also thank Jill Karolyi for the 129/SvJ mice, Denis Duboule for the *Hoxd11* and *Hoxd13* probes, Steve Potter for the *Hoxa11* probe, Greg Dressler for the *Fgf8* probe, and Tom Glaser for our use of the dissecting microscope and camera. We thank Greg Dressler, Mike Glynn and Tom Glaser for the critical reading of the manuscript. L.C.P. was supported in part by a NIH Genetics Training Grant Fellowship. This work was supported by grants from the NIH (HD34059) and the University of Michigan Multipurpose Arthritis and Musculoskeletal Diseases Center (UM-MAC, NIH P60 AR20557).

References

- CONDIE, B.G. and CAPECCHI, M.R. (1993). Mice homozygous for a targeted disruption of *Hoxd-3* (*Hox-4.1*) exhibit anterior transformations of the first and second cervical vertebrae, the atlas, and the axis. *Development* 119: 579-595.
- CONDIE, B.G. and CAPECCHI, M.R. (1994). Mice with targeted disruptions in the paralogous genes *Hoxa-3* and *hoxd-3* reveal synergistic interactions. *Nature* 370: 304-307.
- CONLON, R.A. and HERRMANN, B.G. (1993). Detection of messenger RNA by *in situ* hybridization to postimplantation embryo whole mounts. In *Guide to techniques in mouse development* (Eds. P.M. Wasserman and M.L. DePamphilis), Vol. 225, Academic Press, Inc, San Diego. pp. 373-383.
- CROSSLEY, P. and MARTIN, G.R. (1995). The mouse *Fgf8* gene encodes a family of polypeptides and is expressed in regions that direct outgrowth and patterning in the developing embryo. *Development* 121: 439-451.

- DAVIS, A.P. and CAPECCHI, M.R. (1994). Axial homeosis and appendicular skeleton defects in mice with a targeted disruption of *hoxd-11*. *Development* 120: 2187-2198.
- DAVIS, A.P. and CAPECCHI, M.R. (1996). A mutational analysis of the 5' HoxD genes: dissection of genetic interactions during limb development in the mouse. *Development* 122: 1175-1185.
- DAVIS, A.P., WITTE, D.P., HSIEH-LI, H.M., POTTER, S.S. and CAPECCHI, M.R. (1995). Absence of radius and ulna in mice lacking *Hoxa-11* and *hoxd-11*. *Nature* 375: 791-795.
- DOLLE, P., DIERICH, A., LEMEURE, M., SCHIMMANG, T., SCHUHBAUR, B., CHAMBON, P. and DUBOULE, D. (1993). Disruption of the *Hoxd-13* gene induces localized heterochrony leading to mice with neotenic limbs. *Cell* 75: 431-441.
- DOLLE, P., IZPISUA-BELMONTE, J.-C., BONCINELLI, E. and DUBOULE, D. (1991). The *Hox-4.8* gene is localized at the 5' extremity of the Hox-4 complex and is expressed in the most posterior parts of the body during development. *Mech. Dev.* 36: 3-13.
- FALLON, J.F., LOPEZ, A., ROS, M.A., SAVAGE, M.P., OLWIN, B.B. and SIMANDL, B.K. (1994). FGF-2: Apical ectodermal ridge growth signal for chick limb development. *Science* 264: 104-107.
- FROMENTAL-RAMAIN, C., WAROT, X., MESSADECQ, N., LEMEURE, M., DOLLE, P. and CHAMBON, P. (1996). *Hoxa-13* and *Hoxd-13* play a crucial role in the patterning of the limb autopod. *Development* 122: 2997-3011.
- GANAN, Y., MACIAS, D., DUTERQUE-COQUILLAUD, M., ROS, M.A. and HURLÉ, J.M. (1996). Role of TGF β s and BMPs as signals controlling the position of the digits and the areas of interdigital cell death in the developing chick limb autopod. *Development* 122: 2349-2357.
- GOFF, D.J. and TABIN, C.J. (1997). Analysis of *Hoxd-13* and *Hoxd-11* misexpression in chick limb buds reveals that Hox genes affect both bone condensation and growth. *Development* 124: 627-636.
- HAACK, H. and GRUSS, P. (1993). The establishment of murine Hox-1 expression domains during patterning of the limb. *Dev. Biol.* 157: 410-422.
- HUMMEL, K.P. (1970). *Hypodactyly*, a semidominant lethal mutation in mice. *J. Hered.* 61: 219-220.
- INNIS, J.W., KAZEN-GILLESPIE, K., POST, L.C. and MCGORMAN, J. (1996). High resolution genetic mapping of the *Hypodactyly* (*Hd*) locus on mouse chromosome 6. *Mammal. Genome* 7: 2-5.
- KIMMEL, C.A. and TRAMMEL, C. (1981). A rapid procedure for routine double staining of cartilage and bone in fetal and adult animals. *Stain Technol.* 56: 271-273.
- MACIAS, D., GANAN, Y., SAMPATH, T.K., PIEDRA, M.E., ROS, M.A. and HURLÉ, J.M. (1997). Role of BMP-2 and OP-1 (BMP-7) in programmed cell death and skeletogenesis during chick limb development. *Development* 124: 1109-1117.
- MILAIRE, J. (1992). A new interpretation of the necrotic changes occurring in the developing limb bud paddle of mouse embryos based upon recent observation in four different phenotypes. *Int. J. Dev. Biol.* 36: 169-178.
- MILLER, S., DYKES, D. and POLESKY, H. (1988). A simple salting out procedure for extracting DNA from human nucleated cells. *Nucleic Acids Res.* 16: 1215.
- MOCK, B.A., D'HOOSTELAERE, L.A., MATTHAI, R. and HUPPI, K. (1987). A mouse homeo box gene, *Hox-1.5*, and the morphological locus, *Hd*, map to within 1 cM on chromosome 6. *Genetics* 116: 607-612.
- MORGAN, B.A. and TABIN, C. (1994). Hox genes and growth: early and late roles in limb bud morphogenesis. *Development (Suppl.)*: 181-186.
- MORGAN, B.A., IZPISUA-BELMONTE, J.-C., DUBOULE, D. and TABIN, C.J. (1992). Targeted misexpression of Hox-4.6 in the avian limb bud causes apparent homeotic transformations. *Nature* 358: 236-239.
- MORTLOCK, D.P., POST, L.C. and INNIS, J.W. (1996). The molecular basis of *Hypodactyly* (*Hd*): a deletion in *Hoxa13* leads to arrest of digital arch formation. *Nature Genet.* 13: 284-289.
- NISWANDER, L., TICKLE, C., VOGEL, A., BOOTH, I. and MARTIN, G.R. (1993). FGF-4 replaces the apical ectodermal ridge and directs outgrowth and patterning of the limb. *Cell* 75: 579-587.
- PIZETTE, S. and NISWANDER, L. (1999). BMPs negatively regulate structure and function of the limb apical ectodermal ridge. *Development* 126: 883-894.
- RIJLI, F.M., MATYAS, R., PELLEGRINI, M., DIERICH, A., GRUSS, P., DOLLE, P. and CHAMBON, P. (1995). Cryptorchidism and homeotic transformations of spinal nerves and vertebrae in *Hoxa-10* mutant mice. *Proc. Natl. Acad. Sci. USA* 92: 8185-8189.
- ROBERTSON, K.E., ADAMS, A., TICKLE, C. and DARLING, S.M. (1996). Cellular analysis of limb development in the mouse mutant *Hypodactyly*. *Dev. Genet.* 19: 9-25.
- ROBERTSON, K.E., TICKLE, C. and DARLING, S.M. (1997). *Shh*, *Fgf4* and *Hoxd* gene expression in the mouse limb mutant *Hypodactyly*. *Int. J. Dev. Biol.* 41: 733-736.
- SAUNDERS, J.W. (1948). The proximodistal sequence of origin on the parts of the chick wing and the role of the ectoderm. *J. Exp. Zool.* 108: 363-403.
- SMALL, K.M. and POTTER, S.S. (1993). Homeotic transformations and limb defects in *Hoxa11* mutant mice. *Genes Dev.* 7: 2318-2328.
- SUMMERBELL, D. (1974). A quantitative analysis of the effect of excision of the AER from the chick limb bud. *J. Embryol. Exp. Morphol.* 32: 651-660.
- SUMMERBELL, D., LEWIS, J.H. and WOLPERT, L. (1973). Positional information in chick limb morphogenesis. *Nature* 375: 492-496.
- YOKOUCHI, Y., NAKAZATO, S., YAMAMOTO, M., GOTO, Y., KAMEDA, T., IBA, H. and KUROIWA, A. (1995). Misexpression of *Hoxa-13* induces cartilage homeotic transformation and changes cell adhesiveness in chick limb buds. *Genes Dev.* 9: 2509-2522.
- YOKOUCHI, Y., SAKIYAMA, J.-I., KAMEDA, T., IBA, H., SUZUKI, A., UENO, N. and KUROIWA, A. (1996). BMP-2/-4 mediate programmed cell death in chicken limb buds. *Development* 122: 3725-3734.
- ZAKANY, J., FROMENTAL-RAMAIN, C., WAROT, X. and DUBOULE, D. (1997). Regulation of number and size of digits by posterior Hox genes: a dose-dependent mechanism with potential evolutionary implications. *Proc. Natl. Acad. Sci. USA* 94: 13695-13700.

Received: March, 1999

Accepted for publication: May 1999